POLITECNICO DI TORINO
Repository ISTITUZIONALE

A fault/failure detection algorithm based on a grid of virtual sensors for engine health monitoring

Original
A fault/failure detection algorithm based on a grid of virtual sensors for engine health monitoring / Khan, Al-Amin; Ferlauto, Michele; Yang, Jinguang. - ELETTRONICO. - 2116(2019), p. 450089. ((Intervento presentato al convegno INTERNATIONAL CONFERENCE OF NUMERICAL ANALYSIS AND APPLIED MATHEMATICS (ICNAAM 2018).

Availability:
This version is available at: 11583/2743847 since: 2019-07-29T09:16:07Z

Publisher:
AIP Publishing

Published
DOI:10.1063/1.5114556

(Article begins on next page)

A fault/failure detection algorithm based on a grid of virtual sensors for engine health monitoring

Cite as: AIP Conference Proceedings **2116**, 450089 (2019); https://doi.org/10.1063/1.5114556
Published Online: 24 July 2019

Al-Amin Khan, Michele Ferlauto, and Jinguang Yang

A Fault/Failure Detection Algorithm based on a Grid of Virtual Sensors for Engine Health Monitoring

Al-Amin Khan[1], Michele Ferlauto[2,a)] and Jinguang Yang[3]

[1]*Department of Mathematics, Jahangirnagar University, Savar,Dhaka-1342, Bangladesh*
[2]*Department of Mechanical and Aerospace Engineering, Politecnico di Torino, Turin, Italy*
[3]*School of Energy and Power, Dalian University of Technology, Dalian, China*

[a)]Corresponding author: michele.ferlauto@polito.it

Abstract. A network of virtual sensors from a set of N real sensor is derived by using a model reduction approach. Starting from the output of a real sensor, analytical correlations are derived an used for linking the corresponding set of virtual sensors. By applying this procedure to all real sensors, a matrix of sensors is derived. The system can monitor its health by comparing the sensor outputs and diagnose if a failure is occurring. The application to a sensor system for a jet engine configuration is illustrated.

INTRODUCTION

The continuous expansion of intelligent systems and of multi-purpose Unmanned Aerial Vehicles (UAV) has increased the demand and development of sensor devices with self-diagnostic and prognostic features[1–7], often working in full-authority control systems [9]. Actual trend involves the use of Artificial intelligence in driving vehicles with limited human directives, e.g. drones in formation flight, pathfinders and rovers in space exploration, etc. Moreover, drones are particularly suitable to operate in hostile environments and adverse conditions, where currently the search for human lives endangers that of rescuers.[10–12]. UAVs able to carry out long and dangerous patrols require high power that necessarily relies on thermal engines. Very compact and light jetengines are now available on the market at affordable cost. The management of these engines is far more complex and difficult than battery-powered systems. These minimal power systems must be also equipped with sensor systems adequate to the challenging tasks mentioned above. In modern Full Authority Digital Engine Control (FADEC) units the logic of self-diagnosis and management of errors and faults is by far the functionality that requires the highest computational cost. In the micro jetengines we consider, the main issues still remains that of the higher class engines, e.g. in flight engine relight, control of possible instabilities, thermal issues [13, 14], but the possible control strategies must be simpler, because the power units are reduced to a minimal set of components. To increase reliability and safety of these systems, the autonomous ability of recognize the actual working conditions and to make the required corrections becomes an essential feature. In present paper a procedure based on a minimal set of sensors and the corresponding self-diagnosis logics are illustrated.

MATHEMATICAL MODEL

We take a typical jetengine configuration as reference system. Its steady state conditions are a function of the ambient conditions, of the flight speed and of the control setting. Let us now consider a set of N sensors M_i placed at different axial positions or measuring different physical variables at the same location. Moreover, we assume that for each engine component a real-time model is available, either based on a reduced order model or an empirical correlation. By combining the a single sensor measure with the model equations, an estimation of the system status can be deduced. The system conditions and the setting of controls are known. From the i-th sensor output we can therefore compute a set of estimated values m_{ij} for the output of j-th virtual sensor, with $1 \leq j \leq N$ and $i \neq j$. The result can be represented as a $N \times N$ matrix $\boldsymbol{M}$ as in Figure 1, where boxed elements $m_{ii} = M_i$ represents real sensors, also corresponding to the matrix trace. The remaining elements are hereby called ”virtual” sensors and are estimated row-wise, starting from

International Conference of Numerical Analysis and Applied Mathematics (ICNAAM 2018)
AIP Conf. Proc. 2116, 450089-1–450089-4; https://doi.org/10.1063/1.5114556
Published by AIP Publishing. 978-0-7354-1854-7/$30.00

$$
\begin{bmatrix}
\boxed{M_1} & \longrightarrow & m_{12} & \longrightarrow & m_{13} & \longrightarrow & m_{14} & \longrightarrow & m_{15} \\
m_{21} & \longleftarrow & \boxed{M_2} & \longrightarrow & m_{23} & \longrightarrow & m_{24} & \longrightarrow & m_{25} \\
m_{31} & \longleftarrow & m_{32} & \longleftarrow & \boxed{M_3} & \longrightarrow & m_{34} & \longrightarrow & m_{35} \\
m_{41} & \longleftarrow & m_{42} & \longleftarrow & m_{43} & \longleftarrow & \boxed{M_4} & \longrightarrow & m_{45} \\
m_{51} & \longleftarrow & m_{52} & \longleftarrow & m_{53} & \longleftarrow & m_{54} & \longleftarrow & \boxed{M_5}
\end{bmatrix}
$$

FIGURE 1. matrix representation of the sensor array. Boxes are real sensors, circle are virtual sensors. Arrows show the domain of dependance and of influence of each element.

the the real sensor M_i . Once all the elements are computed, the j-*th* column of the matrix $\boldsymbol{M}$ contains the output of the j-*th* sensor and the estimated output of the N-1 virtual sensors, each one deduced with a different degree of accuracy from the output of the other real sensors. At each column of M, N values for the same variable and at the same station is concerned. An eventual fault or failure of one of the real sensors can be then identified by comparison.

For sake of simplicity, let us assume that the temperatures T_3, T_4, T_5 are monitored with the proposed technique. The engine station are labeled according to Figure 2(a). The real sensors are placed at the corresponding engine axial stations, whereas the virtual sensors output is calculated by means of simple energy and work balances between the three stations

$$(h_4^o - h_3^o) = \Delta H(T_3, T_4, \beta_c, \theta) = (h_4^o - h_b^o - \eta_b H_i) f(\theta) \tag{1}$$

$$L_c(T_3, \beta_c, \theta) = h_3^o - h_2^o \tag{2}$$

$$L_t(T_4, \beta_t, \theta) = h_4^o - h_5^o \tag{3}$$

are reformulated as functions the the temperatures and solved according to the supposed unknown variable. The system must anyway have the knowledge of the actual working conditions and control setup. The setting of

$$\theta = (\frac{T_4^o}{T_2^o} / \frac{T_4^o}{T_2^o}_{des}$$

is therefore known. The matrix reduced $\boldsymbol{M}$ is then

$$\boldsymbol{M} = \begin{bmatrix} T_{33} & T_{34} & T_{35} \\ T_{43} & T_{44} & T_{45} \\ T_{53} & T_{54} & T_{55} \end{bmatrix} \tag{4}$$

As a reminder $T_{33} = T_3$ is the temperature measured by the sensors at station 3, while T_{34}, T_{35} are the temperature at station 4 and 5, respectively, deduced from the measure T_{33}. The other elements of $\boldsymbol{M}$ are deduced accordingly. Each column j of $\boldsymbol{M}$ is composed therefore by a real measure of the temperature T_j and two estimations of it. The straight comparison of these value allow us to make a diagnosis by the following remarks: (i) if the real and virtual sensor outputs closely match, the system is working correctly. (ii)if the virtual sensors are each other in reasonable close agreement and the real one is not, the real sensor may have a faults or a failure. (iii) if the real and one virtual sensor are in close agreement and the second virtual sensor is not, then the real sensor linked of the latter failed.

NUMERICAL EXAMPLE

In the numerical example proposed, we extracted a low order model of the jetengine Pratt&Withney-J85.The model is based on the computation of the engine operating line by using the code GSP[15]. The extracted correlations for the Fuel-Air Ratio (FAR), for the compressor β_c and turbine β_t pressure ratios are shown in Figure 2 as a function of the throttle setup θ. The virtual sensor network is computed by using the relations (1)-(3). A calibration procedure is then applied in order to improve the virtual sensor accuracy over the operative range of the engine.

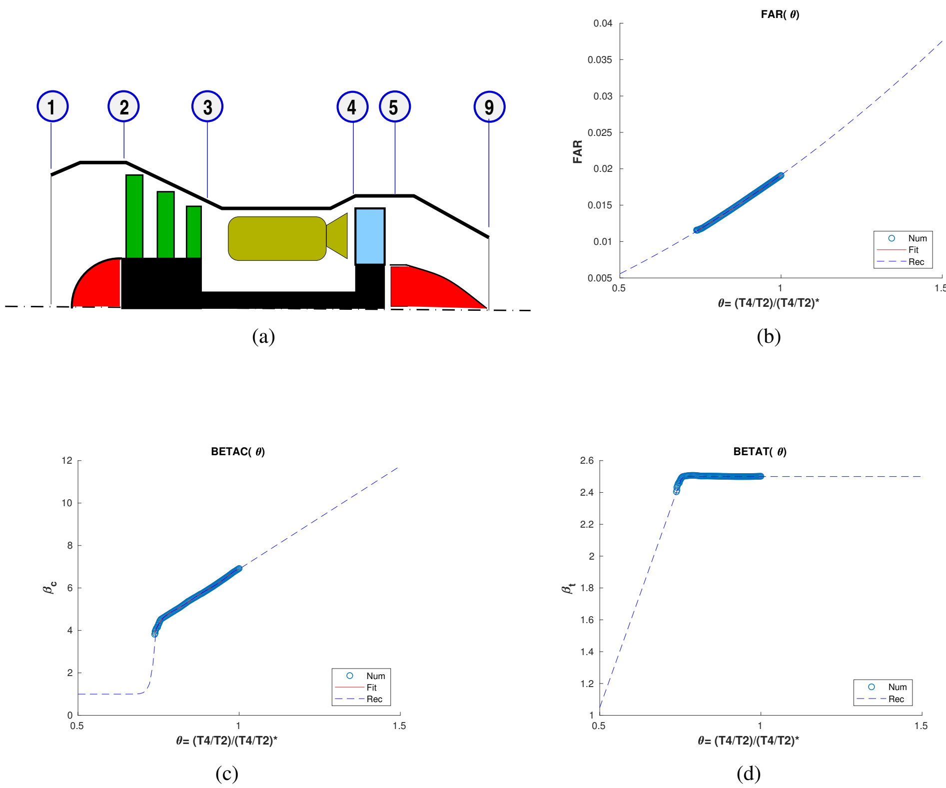

FIGURE 2. Engine reference sections (a) and working line. Diagrams of the Fuel-A-Ratio (b), of the Compressor Pressure Ratio β_c (c) and Turbine Pressure Ratio β_t as a function of the throttle setting θ.

The behavior of the system is simulated numerically as follows. At a generic throttle setting θ, the outputs of the real sensors RS_1, RS_2, RS_3 are based on the corresponding temperatures computed by GSP. A random displacement ΔT is added to each sensor in order to simulate its precision. In order to simulate a possible failure a temperature mismatch is introduced as

$$\Delta T_i = \begin{cases} \alpha * \Delta T^* & \alpha \geq 0.5 \\ 0 & \alpha < 0.5 \end{cases} \tag{5}$$

where α is a random variable, ΔT^* the maximum guessed mismatch at failure. This mismatch is associated to the sensor RS_i only, where i can assume the values 1,2,3 randomly. Let us note that a failure is present only if the random variable $\alpha \geq 0.5$.

At each computation: (i) the sensor outputs are simulated according to the described precision and failure models; (ii) the matrix M is computed and (iii) the sensor outputs are compared in order to identify if and where a failure happened. The system effectiveness has been tested by carrying out a parametric study. The percentage η_1, η_2, η_3 of detected failures of $RS_1, RS_2.RS_3$, respectively, are shown in Figure 3 as a function of the sensitivity setting (ξ_1, ξ_2, ξ_3). For each of the $10 \times 10 \times 10$ ξ-triplets, the statistics of failures is based on 10^5 simulations.

CONCLUSIONS

A numerical framework for the definition of a network of virtual sensors from a set of N real sensor has been described. The method uses a model reduction strategy in order to derive the empirical correlations which link adjacent sensors. From the output of each real sensor a prevision of the output of all other sensors is computed.We defined each single estimation as a ”virtual” sensor. By applying this procedure to all real sensors, a matrix is derived. After applying a calibration for improve the virtual sensors accuracy, an eventual failure of one of the sensors is deduced by comparison. The application to a jet engine configuration has been illustrated.

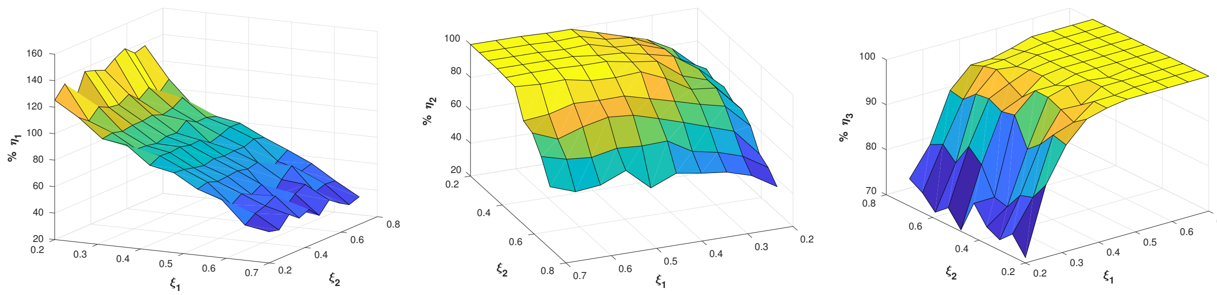

(a) (b) (c)

FIGURE 3. The percentage η_1, η_2, η_3 of detected failures of sensor RS_1 (b), RS_2 (c) and RS_3 (d) as a function of the selected sensitivities (ξ_1, ξ_2, ξ_3).

ACKNOWLEDGMENTS

The financial support of Politecnico di Torino by the SCUDO Research Scholarship "JLAB: a Framework for Experimental Testing, Modeling and Simulation of Gas Turbine Engine Components", by the China Scholarship Council (CSC) and by the National Science Foundation of China (N^o 51606026) are gratefully acknowledged.

REFERENCES

[1] A. Ferrara, S. Sacone, and S. Siri, Advances in Industrial Control 169–190 (2018).

[2] A. Lerro, M. Battipede, P. Gili, and A. Brandl, 6th CEAS Air&Space Conference, Bucarest, (2017).

[3] M. Wright and R. Horowitz, IEEE Transactions on Intelligent Transportation Systems **17**, 3577–3590 (2016).

[4] G. Bartolini, A. Estrada, and E. Punta, IEEE 56th Annual Conference on Decision and Control, Melbourne, Australia 6671–6676 (2017).

[5] A. Provost, G. Bonneric, M. Ferlauto, and G. Di Cicca, 4th IEEE International Workshop on Metrology for AeroSpace, MetroAeroSpace 2017, Padua, Italy 560–564 (2017).

[6] M. Ferlauto and R. Marsilio, *Computational Fluid Dynamics 2006* (Springer Verlag, Berlin, 2009), 573–78.

[7] A. Masiero, F. Fissore, F. Guarnieri A, Pirotti, and A. Vettore, Arch Photogram Rem Sens Spatial Inform Sci **40**, 219–225 (2015).

[8] L.C. Jaw and J.C. Mattingly AIAA Educational Series, Reston, VA (2009).

[9] M. Ferlauto and R. Marsilio, Advances in Aircraft and Spacecraft Science **5**, 349–362 (2018).

[10] L. Marconi, S. Leutenegger, S. Lynen, M. Burri, R. Naldi, and C. Melchiorri, Proceedings of the IEEE International Symposium on Safety, Security, and Rescue Robotics, Linkoping, IEEE (2013).

[11] J. Joern, PhD thesis, University of Denver (2015).

[12] SAR-Drones, "Search with aerial RC multirotor (SWARM)," (2016).

[13] M. Ferlauto, Proc. IMEchE Part A: Journal of Power and Energy **228**, 328–339 (2014).

[14] M. Ferlauto, Inverse Problems in Science and Engineering **21**, 269–282 (2013).

[15] W. Visser, PhD, Thesis, TU-Deft, NL (2015).